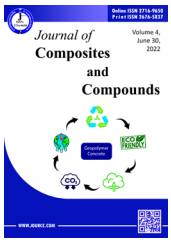

Available online at www.jourcc.com

Journal homepage: www.JOURCC.com

Journal of Composites and Compounds

Molecular imprinted polymer shell on goethite nanorod core for creatinine identification and measurement

*Seyed Mojtaba Amininasab [a] *, Parvin Holakooei [a], Zahed Shami [a], Elham Jaliliyan [a]*

[a] *Department of Chemistry, University of Kurdistan, Sanandaj, Iran*

A B S T R A C T

A new creatinine molecular imprinted polymer on the surface of goethite nanorods (CMIPG) was synthesized using the core-shell structure for the absorption and identification of creatinine. Nano goethite particles (NG) that had been modified with fumaric acid were employed as a core, and a polymerization procedure was carried out in the methacrylic acid (MAA) presence as a functional monomer and creatinine as a template on the surface of the modified goethite nanorods (MGN). Characterization of the CMIPG by energy dispersive spectroscopy-coupled scanning electron microscopy (SEM-EDS), field emission scanning electron microscopy (FESEM), Fourier transform infrared (FT-IR), and thermal gravimetric analysis (TGA) showed that the polymerization was successful. The effect of different factors such as pH, contact time, the amount of the adsorbent, imprinting efficiency, and primary creatinine concentration on creatinine adsorption capacity of CMIPG were evaluated and the results showed that recognition sites were created on the nanoparticles' surface through the polymerization process. The ability of CMIPG for selective identification was studied by the binary solution of creatinine and its analogous such as creatine, L-tyrosine, and N-hydroxysuccinimide (NHS) revealing its ability to selectively absorb creatinine. Moreover, the CMIPG's release and reusability, isotherm, and kinetic models were examined.

Peer review under responsibility of JCC Research Group

A R T I C L E I N F O R M A T I O N

Article history:
Received 25 April 2022
Received in revised form 21 May 2022
Accepted 24 June 2022

Keywords:
Molecular imprinted polymer
Goethite nanorods
Creatinine
Selectivity
UV-vis spectrophotometer

1. Introduction

Creatinine is a byproduct of the muscular contraction mechanism. During this mechanism, creatine and its analogue, phosphocreatine, are tranformed to creatinine [1, 2]. The reference level of creatinine in human serum is 60-130 µM for a male and 0.5-120 µM for a female [3]. Measuring creatinine is the most commonly used indicator of renal function [4]. One of the routine clinical laboratory methods for measuring creatinine is the Jaffe's reaction [5, 6]. The other methods are mass-spectrometry [7], cation-exchange chromatography [8], biosensors [9, 10], high-performance liquid chromatography (HPLC) [11, 12], spectroscopic methods [13], and separation methods including capillary electrophoresis (CE), gas chromatography (GC), and liquid chromatography (LC) [14]. Expensive instruments, difficult stabilization, and immobilization of some biological molecules are the problems of these methods [15]. Today, site-specific polymers for detecting target molecules have attracted much attention. Molecular imprinting is an advanced technique to design specific cavities for various target molecules [16-23]. In molecular imprinted polymers (MIPs), the pore shape, size, and chemical functionality are exactly complementary to the target molecule. Hence, these polymers have molecular memory to select the specific target molecule [24, 25]. Different MIPs are designed to evaluated creatinine adsorption [26, 27].

In order to increase the efficiency of the MIPs and organize their structure, nanoparticles (NPs) such as Fe_3O_4 [28], quantum dots [29], and silica [30] has been used. There are several methods for preparing creatinine MIPs: bulk polymerization [31], sol–gel [32] core–shell techniques [33], etc. Nowadays nanoparticles are commonly used in preparing MIPs due to the high surface-to-volume ratio for adsorbing templates. Thus, the use of nanoparticles has gained the researchers' attention and provides a suitable method for recognizing target molecules in a short time. Because of the unique structure of core–shell MIPs, most of the target molecules stay on the shell surface resulting in better removal of the template and the easier attachment of the template molecule to target sites. This method can thereby lead to a more proper mass transfer [34].

Due to their distinctive chemical compositions, great stability, and low toxicity, iron oxy-hydroxides have demonstrated outstanding adsorption affinity in water systems. Due to its great thermal stability and high mobility, goethite (α-FeOOH) is probably the most common and stable iron oxy-hydroxide polymorph found in natural soils and sediments [35]. Due to its numerous surface hydroxyl groups, it can join with different compounds [36]. Its rod-like crystal structure gives a high level of surface-to-volume ratio. This property causes the adsorption of the template as well [37].

In this article, modified goethite nanoparticles were used for the first time to prepare CMIPG to adsorb and identify creatinine. Non-imprinted

* *Corresponding author: Seyed Mojtaba Amininasab; E-mail: m.amininasab@uok.ac.ir*
https://doi.org/10.52547/jcc.4.2.3

polymer on the surface of goethite nanorods (NIPG) was synthesized in order to determine the imprinting efficiency. The ability of CMIPG to adsorb creatinine in different conditions was also investigated.

2. Materials and methods

2.1. Materials

2, 2′-azobis (isobutyronitrile) (AIBN), Methacrylic acid (MAA), creatinine, N-hydroxysuccinimide (NHS), ethylene glycol dimethacrylate (EGDMA), L-tyrosine, potassium hydroxide (KOH), creatine, fumaric acid, iron (III) nitrate nonahydrate ($Fe(NO_3)_3{\cdot}9H_2O$) and solvents were purchased from Sigma-Aldrich (Germany). Tamin Pharmaceutical Investment Company in Iran provided the polyvinylpyrrolidone (PVP) with Mw of 40000 g/mol (TPICO). Also, analytical grade bases and acids were provided from Sigma–Aldrich (Germany) and utilized without any purification.

2.2. Characterization and instrumentation

TGA analysis (with DuPont Instruments TGA 951 from 25°C to 700 °C in a nitrogen flow with a 10 °C min^{-1} rate of heating) and FT-IR spectra (with Bruker Tensor 27 spectrometer using KBr discs) were used to recognize thermal resistance and functional groups, respectively. A Mighty-8 apparatus was used to perform SEM–EDS (TESCAN Company, Prague). FESEM was employed for the determination of the size of nanoparticles and the surface morphology of produced materials using a Mighty-8 instrument (TESCAN Company, Prague). To evaluate the creatinine concentration in the solutions, a UV-vis spectrophotometer (Cecil Instruments, Cambridge, UK) was used.

2.3. NG synthesis and functionalization

The preparation of the MGNs was conducted in two stages [38]. The initial stage was the preparation of NG with several -OH functional groups. Continuous stirring resulted in the dissolution of 4.85 g of Fe $(NO_3)_{39}H_2O$ in 50 ml of distilled water. The process was followed by adding KOH solution (2.73g in 10 ml H_2O) while vigorously stirring. The KOH solution was used to raise the pH of the final mixture to 12. An ultrasonic bath at 25°C was used for 30 minutes to thoroughly mix and homogenize the mixture. We next dried the precipitates in an oven at 100°C for 75 minutes before filtering, washing, and filtering again. In the second phase, 15 g of NG, 10 g of compound fumaric acid, and 250 ml of distilled water were mixed in an ultrasonic bath followed by refluxing at the boiling point of the mixture for 18 hours. Once the mixture reached ambient temperature and was centrifuged, it was dried for 10 hours at 80 °C in an oven.

2.4. Design and preparation of CMIPG

After mixing 0.5 mmol of creatinine and 2 mmol of MAA in solvents (a mixture of acetonitrile and toluene (3:1)) at room temperature for 30 minutes, hydrogen bonds were formed between creatinine and MAA functional groups and host sites that were specifically designed to accept the creatinine were created. As a final step, the template/MAA solution was supplemented with 0.16 g of PVP and 0.25 mmol of AIBN as an initiator. The reason for selecting MAA as the functional monomer is its carboxylic acid groups that can produce hydrogen bonds with the template. The process of CMIPG formation consisted of interaction between MAA/creatinine complex, cross-linker, MGN as a core, and AIBN as initiator. The blend was placed in an ultrasonicator for 15 minutes. Nitrogen was used for 10 minutes to remove oxygen from the final solution. A 60 °C oil bath was used for 24 hours for the polymerization process. CMIPG was dissolved in distilled water for two hours, and dried in a vacuum oven at 50 °C. For the removal of the template, the resultant particles were extracted using a soxhlet and 24 hours of refluxing methanol. A vacuum oven at 60 °C was used to dry polymer particles. NIPG was synthesized under similar circumstances except adding creatinine to confirm the performance of the CMIPG. Scheme 1 depicts the CMIPG preparation procedure.

2.5. Adsorption study

Effect of different parameters was studies to examine the optimal conditions for adsorption, including pH, the adsorbent amount, the initial concentration of creatinine, and contact time. For example, the impact of pH was tested between 5 to 9 (utilizing adjusted buffer solution by NaOH or HNO_3 solutions), the contact time was considered in the range of 5–45 min, initial concentration of creatinine and amounts of CMIPG were tested in the range of 10 to 500 µM and 5-40 mg, respectively. When one factor changed, the others kept constant at their optimum value. A curve for calibration was created at varied creatinine concentrations using a UV-vis spectrophotometer at λ_{max}=235 nm to determine the equilibrium concentration of adsorbed creatinine. The adsorption capacities (Q, µmol g^{-1}) of CMIPG and NIPG were determined by Eq. (1):

$$Q = \frac{(C_0 - C_f)V}{m} \quad (1)$$

where C_0 (µmol L^{-1}) is the primary concentration of creatinine and C_f (µmol L^{-1}) is the equilibrium creatinine concentrations in solutions; V (L) denotes the volume of the creatinine solution; m (g) is the CMIPG weight. The experiments were repeated three times to ensure that they were repeatable.

2.6. CMIPG imprinting efficiency

In four different concentrations (50, 100, 200, and 400 M), 30 mg of CMIPG and NIPG were added to a 10 ml creatinine solution. Polymer particles were collected via filtration after 20 minutes of stirring. Using a calibration curve, the concentration of the remaining creatinine was calculated from the maximum adsorption of creatinine at λ_{max} = 235 nm.

2.7. Creatinine release and reusability of CMIPG

To learn more about CMIPG's desorption qualities, the study examined its reusability and release. In order to study the release ability, 30 mg of loaded CMIPG were stirred in 10 ml methanol. After 20 min, the CMIPG particles were collected by filtering, dried, and eventually subjected to fresh methanol. The release experiment was repeated 3 times. A UV-vis spectrophotometer was utilized to determine the amount of isolated creatinine in the release medium. 30 mg of CMIPG was added to a 10 ml creatinine solution at a concentration of 200 µM to test its reusability. At ambient temperature, the blend was stirred for 20 minutes. Filtering was used to collect the loaded CMIPG. CMIPG was poured into methanol to extract creatinine, and the dried CMIPG was employed four times in the adsorption-desorption cycle. UV-vis spectra were used to determine the amount of adsorbed creatinine in each cycle.

2.8. Selectivity and competitive adsorption of CMIPG

Three structural mimics, such as NHS, L-tyrosine, and creatine were used to quantify the amount of loaded creatinine in their presence for interference studies and to examine the CMIPG selectivity. Four solutions of creatinine/creatine, creatinine, creatinine/L-tyrosine, and creatinine/NHS were tested (10 mL of four 200 µM solutions). Then, in each of these four solutions, 30 mg of CMIPG was added. At room temperature, each solution was stirred for 20 minutes. The concentration of adsorbed

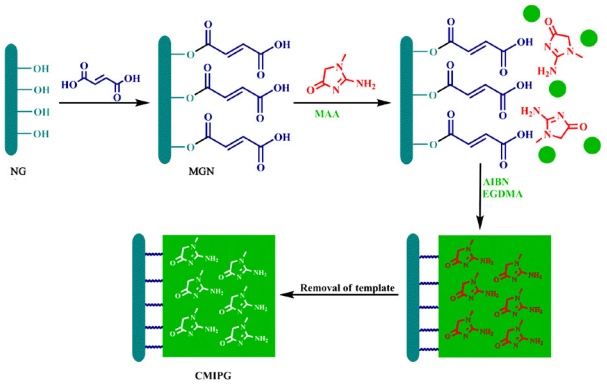

Scheme. 1. Preparation steps of CMIPG.

creatinine was evaluated via a UV-vis spectrophotometer after the binding equilibrium was achieved. Equation 2 and 3 were used to calculate the selectivity coefficients of creatinine and distribution in relation to its analogues:

$$K_d = \frac{(C_0 - C_f)}{C_f}(V/m) \quad (2)$$

$$K = \frac{K_d(template\ creatinine)}{K_d(\text{int}erferent\ \ creatinine)} \quad (3)$$

where K_d denotes distribution coefficient and K represents the selectivity coefficients ; C_0 and C_f denote the primary and equilibrium concentrations of creatinine in the solution (μmol L^{-1}); m is the CMIPG mass (g); V stands for the solution volume (L). The remained creatinine concentration in solution was calculated by adsorption amount of creatinine in maximum adsorption at λ_{max} = 235 nm evaluated by the use of a calibration curve via UV-spectrophotometer. All examinations were done three times to make sure that they were repeatable. As illustrated in Fig. 1, the creatinine chemical structure and its relevant molecules could be seen.

3. Results and discussion

3.1. Characterization of CMIPG

The FT-IR spectra of NG, MGN, and CMIPG are shown in Figure 2. The Fe–O stretching vibration is associated with the adsorption band at around 638 cm^{-1} in the NG spectrum, while the –OH groups on the surface of NG are presented by the broad adsorption band at ~3500 cm^{-1}. The Fe-O-OH vibration in NG is related to the particular and sharp bands at 892 cm^{-1} and 794 cm^{-1}. Stretching vibrations at 1604 cm^{-1} in the MGN spectrum are related to the C=C band and confirm the formation of modified nanoparticles. C=O and C-O ester bonding were attributed to the adsorption bands at 1731 cm^{-1} and 1151 cm^{-1}, respectively, and were indications of CMIPG production. An aliphatic stretching vibration peak was visible at 2958 cm^{-1}. The elimination of the characteristic band of creatinine in the FT-IR spectra of CMIPG can confirm the complete removal of creatinine from CMIPG.

The FESEM images of NG, MGN, and CMIPG show their morphological properties (Fig. 3). The FESEM image of the NG (Fig. 3a) showed rod-like morphology and a mean particle size of ~72 nm. The micrographs of MGN illustrate uniform regular shapes (Fig. 3b). Regular morphology was clear for CMIPG in Fig. 3c, which demonstrated core-shell structure. The results of EDS analysis of MGN and CMIPG (Fig. 3d and 3e) showed that the C and O peaks are present in the MGN spectrum (Fig. 3d) revealing a successful functionalization of nanoparticles. The Fe, C, and O peaks in Fig. 3e, demonstrates the presence of

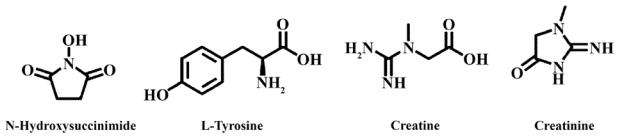

Fig. 1. NHS, creatinine, L-tyrosine, and creatine molecular structures.

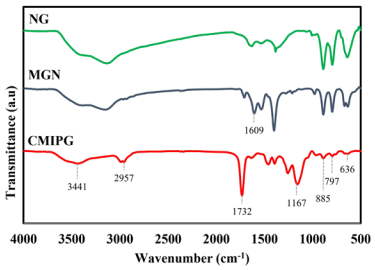

Fig. 2. FT-IR spectrum of NG, MGN, CMIPG.

MGN in the CMIPG structure. Also, the absence of nitrogen ensures that creatinine was removed.

The TGA curves of NG, MGN, and CMIPG are plotted in Fig. 4. In the TGA curve of NG, 15% weight loss at 250 °C can be due to the surface humidity and the char-yield was about 85% at 700 °C. The 30% weight loss of the MGN from 200-400 °C could be related to the degradation of the organic compounds on the surface of NPs. About 55% weight loss at ~450 °C in TGA curve of CMIPG was observed and ~40% of the initial weight was remained at 700 °C.

3.2. Optimum adsorption time determination

As observed in Fig. 5a, the creatinine absorption capacity of CMIPG changes with time. In this study, 30 mg CMIPG was in touch with 10 ml of creatinine solution (200 μM) at ambient temperature for 5-45 min. The adsorption capacity of CMIPG was improved by increasing the contact duration up to 20 minutes (97 %) and then it became constant. As a result, 20 minutes was regarded as the optimum time for creatinine to be absorbed.

3.3. Evaluation of pH effect on creatinine adsorption

In order to achieve the optimum pH as a vital factor for creatinine adsorption by the CMIPG, the influence of pH (in the range of 5-9) on the adsorption of CMIPG was examined using 30 mg of CMIPG in contact with creatinine solution (200 μM) for 20 min. The results (Fig. 5b)

Table 1.
Isothermal correlation coefficients at room temperature (pH of 7).

Isotherm models	Parameters	
Langmuir	$1/Q_mK_L$ (g L^{-1})	0.04
	R^2	0.99
Temkin	A (L g^{-1})	0.11
	B	0.91
	R^2	0.88
Freundlich	K_f	3.13
	n	2.77
	R^2	0.83
Redlich–Peterson	K_R	0.77
	α_R	0.38
	β	-
	R^2	0.74

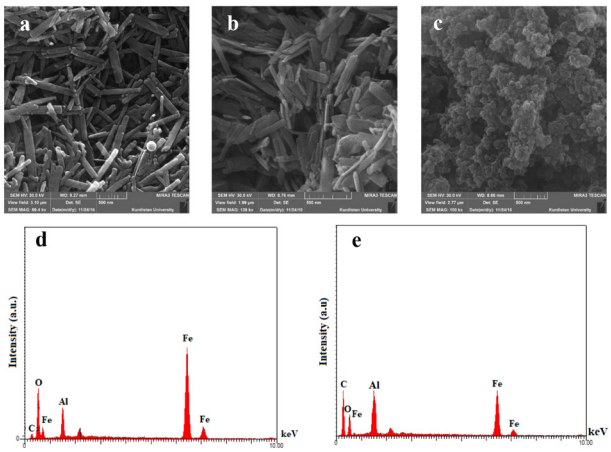

Fig. 3. FESEM micrographs of (a) NG, (b) MGN, and (c) CMIPG, EDS images of (d) MGN, (e) CMIPG.

showed that the adsorption capacity of creatinine was not different in acidic and basic pHs. According to these results, the optimum pH was at pH=7, which is close enough to the pH of biological systems. Thus, the pH of all measurements was kept at 7.

3.4. Effect of CMIPG mass on creatinine adsorption

To study the impact of the CMIPG mass, different amounts of CMIPG (5-40 mg) were exposed to 200 µM creatinine. Results showed maximum adsorption of creatinine was achieved by using 30 mg of CMIPG in the adsorption procedure. Thus, 30 mg of CMIPG was used in the next optimization steps.

3.5. Isotherm studies (Effect of creatinine concentration)

MIP adsorption is greatly influenced by the initial concentration of the template. For this purpose, different concentrations of creatinine solution (10 ml of 10-500 µM) at pH=7 were mixed with 30 mg of CMIPG for 20 min. After filtering the adsorbent particles, the adsorbed creatinine was measured (Fig. 5c**)**. It is clear that increasing the creatinine concentration from 10 to 200 µM leads to an increase in CMIPG adsorption capability (about 100 %). It means that the maximum adsorption occurred at 200 µM of creatinine concentration. For all concentrations (50,100,200,400 µM), the equilibrium adsorption capacity (Q µmol g^{-1}) for CMIPG and NIPG was calculated (equation 1) and imprinting efficiency was determined by dividing absorbed creatinine amount by CMIPG to the adsorbed creatinine by NIPG. As Fig. 5d shows, the maximum adsorption of NIPG was in a concentration of 50-100 µM (about 57%) and after that, it decreased. However, the adsorption values for CMIPG at 50-100 µM were about 96%. Thus, the adsorption capacity of CMIPG is high due to the selective adsorption sites in the CMIPG structure. The imprinting efficiency, in 50, 100, 200, 400 µM concentrations of creatinine were 1.6, 1.8, 4.1, and 5.9, respectively. It can be concluded that the presence of template during the polymerization process creates selective sites for the creatinine identification.

To study binding parameters in the adsorption process, isotherm equations such as Langmuir (Equation. (4)), Temkin (Equation (5)), Freundlich (Equation (6)), and Redlich–Peterson (Equation (7) were used.

Table 2.
CMIPG selectivity

Substrate	Q (µmol/g)	C_0-C_f (µmol/L)	Competitive Loading (%)	K_d (L/g)	K
Creatinine	64.66	194	97	10.77	-
Creatinine/Creatine	63.64	190.92	95.46	7.00	1.53
Creatinine/NHS	61.26	183.78	91.89	3.77	2.85
Creatinine/L-tyrosine	64.29	192.89	96.44	9.04	1.19

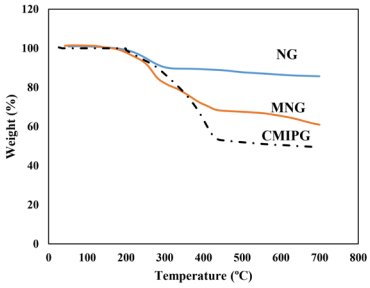

Fig. 4. The TGA plots of NG, MGN, and CMIPG.

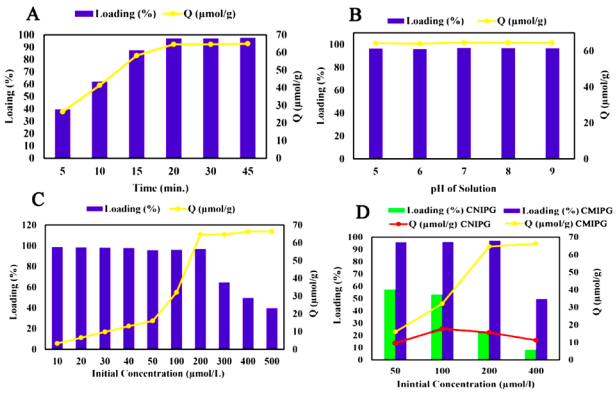

Fig. 5. Adsorption capacity variations with (a) time, (b) pH (30 mg of CMIPG, 200 µmol/L creatinine), (c) beginning concentration of creatinine, and (d) imprinting efficiency of CMIPG and NIPG.

$$\frac{C_e}{Q_e} = \frac{1}{Q_m K_L} + \frac{C_e}{Q_m} \quad (4)$$

$$Q_e = B\ln(A) + B\ln(C_e) \quad (5)$$

$$\ln Q_e = \ln K_f + \frac{1}{n}\ln C_e \quad (6)$$

$$\frac{C_e}{Q_e} = \frac{1}{K_R} + \frac{\alpha_R}{K_R} C_e^{\beta} \quad (7)$$

where C_e is the equilibrium concentration of creatinine (µmol L^{-1}); the adsorption amount at the equilibrium (µmol g^{-1}) is denoted by Q_e; Q_m stands for the maximum capacity of adsorption of CMIPG (µmol g^{-1}). The Langmuir constant related to the adsorption energy is K_L and K_f is Freundlich constants that show the capacity of adsorption. K_L and Q_m are obtained from the linear plot slope and intercept of C_e/Q_e against C_e.

Table 3.
Kinetic parameters at pH of 7.0 and room temperature

kinetic model	parameters	
pseudo-first-order	Q_e (mg g^{-1})	3.88
	K_1 (min^{-1})	0.05
	R^2	0.54
pseudo-second-order	Q_e (mg g^{-1})	8.90
	K_2 (g mg^{-1} min^{-1})	0.015
	R^2	0.97
Elovich equation	α (mg g^{-1} min^{-1})	2.17
	β (g mg^{-1})	0.46
	R^2	0.85
Weber–Morris intraparticle diffusion	K_p (mg g^{-1} $min^{-1/2}$)	0.96
	C	1.86
	R^2	0.73

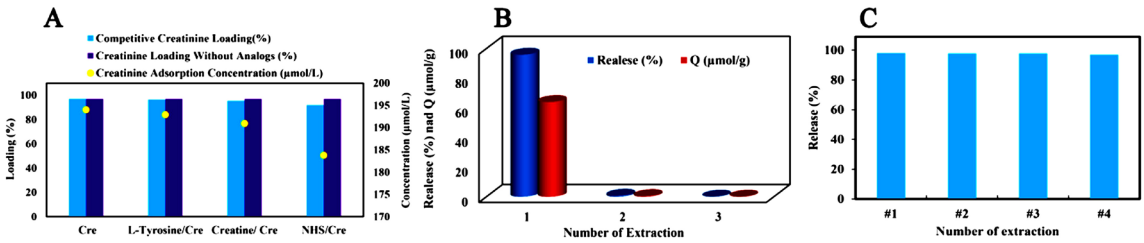

Fig. 6. (A) The creatinine selectivity by CMIPG in the presence of creatine, NHS, and L-tyrosine, (B) creatinine released from CMIPG, and (C) reusability of CMIPG.

K_f and n are obtained by fitting a linear plot of lnQ_e vs. lnC_e. The value obtained for the coefficient of determination (R^2) of each equation (Table 1) showed that the experimental data complied with Langmuir equation and the behavior of CMIPG adsorption was explainable by this equation.

3.6. Evaluation of the CMIPG selectivity in binary mixtures

To observe the selectivity behavior of CMIPG in creatinine adsorption, NHS, creatine, and L-tyrosine were selected as creatinine analogues. Creatinine adsorption was studied in the presence of these analogues (Fig. 6A). The results showed that CMIPG selectively adsorbed creatinine in the presence of the analogues. Interferences of each material led to the decrease in the creatinine amount adsorbed by CMIPG. The CMIPG's selectivity for creatinine considering the individual interference was determined by dividing the amount of adsorbed creatinine by the amount adsorbed by the individual interference (Table 2). The results demonstrated imprinting efficiency. Accordingly, CMIPG act selectively in the adsorption of creatinine because the cavities formed during the imprinting process are similar in size and shape to creatinine.

3.7. CMIPG release and reusability

To identify the desorption ability of CMIPG, the release and reusability of CMIPG were tested (Fig. 6b, c). In this regard, the CMIPG containing creatinine was washed with methanol for 20 min. Determining the total amount of adsorbed creatinine extracted by methanol from CMIPG by the first extraction and after second and third extractions showed that it contained no creatinine. Thus, CMIPG showed good release ability (Fig. 6b).

To understand the reusability of the CMIPG, after each adsorption, CMIPG was used again up to 4 times. The results showed that the adsorption by CMIPG was 97% after four desorption-adsorption cycles (Fig. 6c).

3.8. Studies of adsorption kinetics

Adsorption kinetics of CMIPG was studied from 5 to 45 min in creatinine concentration of 200 µM. As demonstrated in Fig. 5a**,** the binding capacity was increased with the increment of time and the binding equilibrium was achieved at 20 minutes. The relatively high adsorption capacity of CMIPG demonstrated the presence of selective sites on the CMIPG surface for creatinine recognition. To specify the adsorption mechanism of CMIPG, the models containing pseudo-first-order (equation 8) pseudo-second-order (equation 9), the Elovich (equation 10), and Weber-Morris (equation 11) are used to analyze the experimental equilibrium data.

$$\log(Q_e - Q_t) = \log Q_e - \frac{k_1}{2.303}t \quad (8)$$

$$\frac{t}{Q_t} = \frac{1}{k_2 Q_e^2} + \frac{1}{Q_e}t \quad (9)$$

$$Q_t = \frac{1}{\beta}\ln(\alpha\beta) + \frac{1}{\beta}\ln t \quad (10)$$

$$Q_t = K_p t^{\frac{1}{2}} + C \quad (11)$$

where Q_t and Q_e (µmol g^{-1}) represent the adsorbed creatinine amount at various times and at equilibrium, respectively. The rate constants containing, k_2, k_1, α, β, C, Q_e and K_p are obtained by the corresponding slopes and intercepts of linear plots. To find a kinetic model for the adsorption of creatinine, kinetic parameters and the coefficient of determination (R^2) of all plots were calculated (Table 3**)**. As can be seen, R^2 was 0.97 for pseudo-second-order; thus, the pseudo-second-order model explains the creatinine adsorption mechanism.

4. Conclusions

A novel molecular imprinted polymer shell on goethite nanorod core was synthesized for selective creatinine detection. In the presence of MAA (functional monomer), EGDMA (cross-linker), and functionalized nanoparticles, a radical polymerization process was carried out. Different methods such as EDS, FT-IR, TGA, and FESEM were used to characterize CMIPG. FT-IR and EDS showed that the core-shell structure was successfully achieved. TGA showed thermal resistance and FESEM confirmed a regular shape of CMIPG in size of 72 nm and spherical morphology. The selectivity was investigated by using a binary solution of creatinine and its analogues (NHS, L-tyrosine, and creatine). The value of *K*, for binary solution of creatinine/L-tyrosine, creatinine/NHS, and creatinine/creatine was obtained 1.53, 2.85, and 1.19, respectively. Optimum time for creatinine adsorption was achieved at 20 min. A pseudo-second-order kinetic model and a Langmuir isotherm model both verified the experimental results by using R^2 values. It was shown that at a creatinine initial concentration of 200 µmol L^{-1}, the capacity of adsorption reached its maximum (64.66 µmol g^{-1}). According to the results, CMIPG demonstrated exceptional properties for the detection of creatinine because of selective cavities on CMIPG's surface.

REFERENCES

[1] C. Miura, N. Funaya, H. Matsunaga, J. Haginaka, Monodisperse, molecularly imprinted polymers for creatinine by modified precipitation polymerization and their applications to creatinine assays for human serum and urine, Journal of pharmaceutical and biomedical analysis 85 (2013) 288-294.

[2] M. Wyss, R. Kaddurah-Daouk, Creatine and creatinine metabolism, Physiological reviews 80(3) (2000) 1107-1213.

[3] T.-J. Li, P.-Y. Chen, P.-C. Nien, C.-Y. Lin, R. Vittal, T.-R. Ling, K.-C. Ho, Preparation of a novel molecularly imprinted polymer by the sol–gel process for sensing creatinine, Analytica chimica acta 711 (2012) 83-90.

[4] J. Yu, Y. Wu, S. Wang, X. Ma, The preparation of cellulose nitrate derivatives and their adsorption properties for creatinine, Carbohydrate polymers 70(1) (2007) 8-14.

[5] H.-A. Tsai, M.-J. Syu, Synthesis of creatinine-imprinted poly (β-cyclodextrin) for the specific binding of creatinine, Biomaterials 26(15) (2005) 2759-2766.

[6] K. Spencer, Analytical reviews in clinical biochemistry: the estimation of creatinine, Annals of clinical biochemistry 23(1) (1986) 1-25.

[7] R. Hušková, P. Chrastina, T. Adam, P. Schneiderka, Determination of creatinine in urine by tandem mass spectrometry, Clinica Chimica Acta 350(1) (2004) 99-106.

[8] Y. Yokoyama, S. Horikoshi, T. Takahashi, H. Sato, Low-capacity cation-exchange chromatography of ultraviolet-absorbing urinary basic metabolites using a reversed-phase column coated with hexadecylsulfonate, Journal of Chromatogra-

phy A 886(1) (2000) 297-302.
[9] S. Yadav, A. Kumar, C. Pundir, Amperometric creatinine biosensor based on covalently coimmobilized enzymes onto carboxylated multiwalled carbon nanotubes/polyaniline composite film, Analytical biochemistry 419(2) (2011) 277-283.
[10] W. Sant, P. Temple-Boyer, E. Chanié, J. Launay, A. Martinez, On-line monitoring of urea using enzymatic field effect transistors, Sensors and Actuators B: Chemical 160(1) (2011) 59-64.
[11] I.D. Merás, A.E. Mansilla, M.J.R. Gómez, Determination of methotrexate, several pteridines, and creatinine in human urine, previous oxidation with potassium permanganate, using HPLC with photometric and fluorimetric serial detection, Analytical biochemistry 346(2) (2005) 201-209.
[12] D. Tsikas, A. Wolf, A. Mitschke, F.-M. Gutzki, W. Will, M. Bader, GC–MS determination of creatinine in human biological fluids as pentafluorobenzyl derivative in clinical studies and biomonitoring: inter-laboratory comparison in urine with Jaffé, HPLC and enzymatic assays, Journal of Chromatography B 878(27) (2010) 2582-2592.
[13] J.L. Pezzaniti, T.-W. Jeng, L. McDowell, G.M. Oosta, Preliminary investigation of near-infrared spectroscopic measurements of urea, creatinine, glucose, protein, and ketone in urine, Clinical biochemistry 34(3) (2001) 239-246.
[14] E. Mohabbati-Kalejahi, V. Azimirad, M. Bahrami, A. Ganbari, A review on creatinine measurement techniques, Talanta 97 (2012) 1-8.
[15] T. Sergeyeva, L. Gorbach, E. Piletska, S. Piletsky, O. Brovko, L. Honcharova, O. Lutsyk, L. Sergeeva, O. Zinchenko, A. El'skaya, Colorimetric test-systems for creatinine detection based on composite molecularly imprinted polymer membranes, Analytica chimica acta 770 (2013) 161-168.
[16] H. Huang, C. Zhang, L. Liu, Z. Wang, Synthesis and characterization of a novel quercetin magnetic molecularly imprinted polymer via reversible addition fragmentation chain transfer strategy, Journal of Macromolecular Science, Part A 54(7) (2017) 446-451.
[17] C. Mercy Philip, B. Mathew, Design of EGDMA-Crosslinked Theophylline Imprinted Polymer with High Specificity and Selectivity, Journal of Macromolecular Science, Part A: Pure and Applied Chemistry 45(4) (2008) 335-343.
[18] X.-H. Wang, L. Tang, F.-F. Yang, L.-L. Ying, Y.-P. Huang, Z.-S. Liu, Green synthesis of water-compatible and thermo-responsive molecularly imprinted nanoparticles, European Polymer Journal 92 (2017) 174-184.
[19] W. Huang, Y. Kong, W. Yang, X. Ni, N. Wang, Y. Lu, W. Xu, Preparation and characterization of novel thermosensitive magnetic molecularly imprinted polymers for selective recognition of norfloxacin, Journal of Polymer Research 23(5) (2016) 94.
[20] Z. Wang, T. Qiu, L. Guo, J. Ye, L. He, X. Li, The synthesis of hydrophilic molecularly imprinted polymer microspheres and their application for selective removal of bisphenol A from water, Reactive and Functional Polymers 116 (2017) 69-76.
[21] H.-S. Byun, D.-S. Yang, S.-H. Cho, Synthesis and characterization of high selective molecularly imprinted polymers for bisphenol A and 2, 4-dichlorophenoxyacetic acid by using supercritical fluid technology, Polymer 54(2) (2013) 589-595.
[22] K. Hemmati, A. Masoumi, M. Ghaemy, Tragacanth gum-based nanogel as a superparamagnetic molecularly imprinted polymer for quercetin recognition and controlled release, Carbohydrate polymers 136 (2016) 630-640.
[23] N. Gündoğdu, M. Coşkun, Kinetic study for adsorption of α-naphtholphthalein onto silica gel surface-imprinted polymer and non-imprinted polymer, Journal of Macromolecular Science, Part A 53(12) (2016) 734-740.
[24] A. Suksuwan, L. Lomlim, F.L. Dickert, R. Suedee, Tracking the chemical surface properties of racemic thalidomide and its enantiomers using a biomimetic functional surface on a quartz crystal microbalance, Journal of Applied Polymer Science 132(30) (2015).
[25] K. Matsumoto, B.D.B. Tiu, A. Kawamura, R.C. Advincula, T. Miyata, QCM sensing of bisphenol A using molecularly imprinted hydrogel/conducting polymer matrix, Polymer Journal 48(4) (2016) 525-532.
[26] A.A. Topçu, N. Bereli, İ. Albayrak, A. Denizli, Creatinine imprinted poly (hydroxyethyl methacrylate) based cryogel cartridges, Journal of Macromolecular Science, Part A 54(8) (2017) 495-501.
[27] K. Sreenivasan, R. Sivakumar, Interaction of molecularly imprinted polymers with creatinine, Journal of applied polymer science 66(13) (1997) 2539-2542.
[28] M. Hassanzadeh, M. Ghaemy, An effective approach for the laboratory measurement and detection of creatinine by magnetic molecularly imprinted polymer nanoparticles, New Journal of Chemistry 41(6) (2017) 2277-2286.
[29] H.-Y. Lin, M.-S. Ho, M.-H. Lee, Instant formation of molecularly imprinted poly (ethylene-co-vinyl alcohol)/quantum dot composite nanoparticles and their use in one-pot urinalysis, Biosensors and Bioelectronics 25(3) (2009) 579-586.
[30] Q.Y. Ang, M.H. Zolkeflay, S.C. Low, Configuration control on the shape memory stiffness of molecularly imprinted polymer for specific uptake of creatinine, Applied Surface Science 369 (2016) 326-333.
[31] M. Subat, A.S. Borovik, B. König, Synthetic creatinine receptor: imprinting of a Lewis acidic zinc (II) cyclen binding site to shape its molecular recognition selectivity, Journal of the American Chemical Society 126(10) (2004) 3185-3190.
[32] H.-A. Tsai, M.-J. Syu, Preparation of imprinted poly (tetraethoxysilanol) sol–gel for the specific uptake of creatinine, Chemical engineering journal 168(3) (2011) 1369-1376.
[33] B. Gao, Y. Li, Z. Zhang, Preparation and recognition performance of creatinine-imprinted material prepared with novel surface-imprinting technique, Journal of Chromatography B 878(23) (2010) 2077-2086.
[34] M. Niu, C. Pham-Huy, H. He, Core-shell nanoparticles coated with molecularly imprinted polymers: a review, Microchimica Acta 183(10) (2016) 2677-2695.
[35] M.A. Amrani, A.M. Ghaleb, A. E. Ragab, M.Z. Ramadan, T.M. Khalaf, Low-cost goethite nanorods for As (III) and Se (VI) removal from water, Applied Sciences 10(20) (2020) 7237.
[36] Z. Wang, Y. Ma, H. He, C. Pei, P. He, A novel reusable nanocomposite: FeOOH/CBC and its adsorptive property for methyl orange, Applied Surface Science 332 (2015) 456-462.
[37] E. Brok, C. Frandsen, D.E. Madsen, H. Jacobsen, J. Birk, K. Lefmann, J. Bendix, K. Pedersen, C. Boothroyd, A. Berhe, Magnetic properties of ultra-small goethite nanoparticles, Journal of Physics D: Applied Physics 47(36) (2014) 365003.
[38] J. Rose, M.M. Cortalezzi-Fidalgo, S. Moustier, C. Magnetto, C.D. Jones, A.R. Barron, M.R. Wiesner, J.-Y. Bottero, Synthesis and characterization of carboxylate− FeOOH nanoparticles (ferroxanes) and ferroxane-derived ceramics, Chemistry of Materials 14(2) (2002) 621-628.